Ultrafast dynamics of pyrrolidinium cation ionic liquids

Hideaki Shirota
Department of Chemistry & Chemical Biology, Rutgers, The State University of New Jersey, Piscataway, New Jersey 08854-8087

Alison M. Funston[a] and James F. Wishart
Brookhaven National Laboratory, Chemistry Department, Upton, New York 11973-5000

Edward W. Castner, Jr.
Department of Chemistry & Chemical Biology, Rutgers, The State University of New Jersey, Piscataway, New Jersey 08854-8087

(Received 3 January 2005; accepted 23 February 2005; published online 10 May 2005)

We have investigated the ultrafast molecular dynamics of five pyrrolidinium cation room temperature ionic liquids using femtosecond optical heterodyne-detected Raman-induced Kerr effect spectroscopy. The ionic liquids studied are *N*-butyl-*N*-methylpyrrolidinium bis(trifluoromethylsulfonyl)imide (P_{14}^+/NTf_2^-), *N*-methoxyethyl-*N*-methylpyrrolidinium bis(trifluoromethylsulfonyl)imide (P_{1EOE}^+/NTf_2^-), *N*-ethoxyethyl-*N*-methylpyrrolidinium bis(trifluoromethylsulfonyl)imide (P_{1EOE}^+/NTf_2^-), *N*-ethoxyethyl-*N*-methylpyrrolidinium bromide P_{1EOE}^+, and *N*-ethoxyethyl-*N*-methylpyrrolidinium dicyanoamide (P_{1EOE}^+/DCA^-). For comparing dynamics among the five ionic liquids, we categorize the ionic liquids into two groups. One group of liquids comprises the three pyrrolidinium cations P_{14}^+, P_{1EOM}^+, and P_{1EOE}^+ paired with the NTf_2^- anion. The other group of liquids consists of the P_{1EOE}^+ cation paired with each of the three anions NTf_2^-, Br^-, and DCA^-. The overdamped relaxation for time scales longer than 2 ps has been fit by a triexponential function for each of the five pyrrolidinium ionic liquids. The fast (~2 ps) and intermediate (~20 ps) relaxation time constants vary little among these five ionic liquids. However, the slow relaxation time constant correlates with the viscosity. Thus, the Kerr spectra in the range from 0 to 750 cm^{-1} are quite similar for the group of three pyrrolidinium ionic liquids paired with the NTf_2^- anion. The intermolecular vibrational line shapes between 0 and 150 cm^{-1} are fit to a multimode Brownian oscillator model; adequate fits required at least three modes to be included in the line shape. © *2005 American Institute of Physics*. [DOI: 10.1063/1.1893797]

I. INTRODUCTION

Room temperature ionic liquids (RTILs) are molten salts for which the low temperature limit of the broad liquidus is at or below ambient temperature. The strong electrical interactions in these liquids cause them to have very low vapor pressures, which result in solvent properties that are favorable for "green" chemistry.[1] RTIL vapor pressures are orders of magnitude lower than for neutral organic solvents. RTILs show high solubility for both inorganic and organic compounds, including peptides, proteins, and enzymes. As replacements for volatile organic solvents, the low vapor pressures of RTILs provide opportunities for reducing emissions of volatile organic compounds to the atmosphere.[2–10] In particular the low vapor pressures of RTILs also provide opportunities for reducing the risk of uncontrolled gas phase chain reactions, fires, and explosions. Many important chemical reactions, such as hydrogenations,[11,12] oxidations,[13] and coupling reactions[14,15] have been investigated in RTILs to test their use as organic solvent replacements. RTILs have also proven useful as solvents for materials synthesis,[16] enzymatic catalysis,[17] and enantiomeric synthesis.[18,19] Analytical applications of ionic liquids include uses such as stationary phases for chiral separations,[20] and as nonvolatile solvents for matrix assisted laser desorption ionization time-of-flight mass spectroscopy.[21–23] Each of these applications can benefit from a detailed physical understanding of the dynamics and interactions in ionic liquids. Thus, we have undertaken a spectroscopic study of five pyrrolidinium-cation ionic liquids.

Femtosecond optical heterodyne-detected Raman-induced Kerr effect spectroscopy (OHD-RIKES) is a nonlinear optical polarization technique that measures the depolarized Raman signal from a transparent condensed phase sample in the time domain.[24,25] Using OHD-RIKES, we can measure the dynamics in condensed phases on time scales ranging from 20 fs to 1 ns. The time domain data are converted to the low-frequency depolarized Raman spectrum by direct Fourier transform deconvolution.[25–27] Spectral sensitivity in the range from 0.1 to 750 cm^{-1} makes OHD-RIKES a powerful tool to investigate the intermolecular dynamics and interactions in condensed phases. Recently, femtosecond OHD-RIKES has been used for simple molecular liquids,[24,25,28–30] and for more complex condensed phases

[a]Current address: School of Chemistry, The University of Melbourne, Victoria, 3010 Australia.

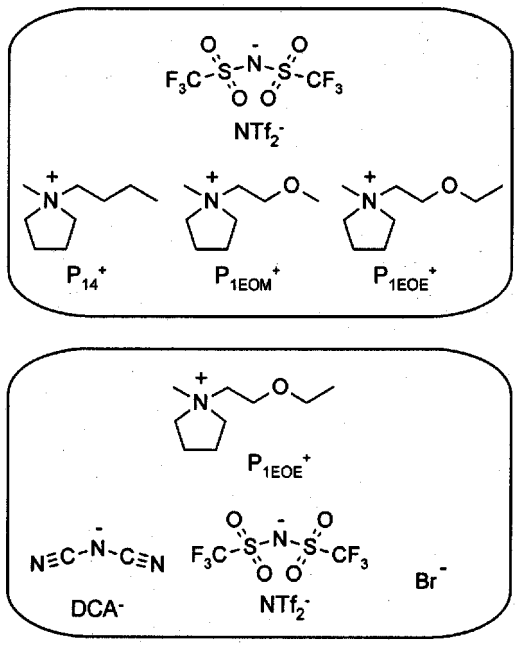

FIG. 1. Chemical structures of the pyrrolidinium cation ionic liquids used in this study. P_{14}^{+} is *N*-butyl-*N*-methylpyrrolidinium cation, P_{1EOM}^{+} is *N*-methoxyethyl-*N*-methylpyrrolidinium cation, P_{1EOE}^{+} is *N*-ethoxyethyl-*N*-methyl-pyrrolidinium cation, NTf_2^{-} is bis(trifluoromethylsulfonyl)imide anion, DCA^{-} is dicyanoamide anion, and Br^{-} is bromide anion.

such as nanoporous glasses,[31,32] microemulsions,[33,34] hydrated peptide and protein solutions,[35–37] and polymer solutions.[34,38]

Several groups have studied the ultrafast dynamics of aromatic imidazolium ionic liquids using OHD-RIKES. Quitevis and co-workers characterized how changes of the alkyl substituent affected the intermolecular vibrational dynamics for a series of 1-alkyl-3-methylimidazolium cations paired with bis(trifluoromethylsulfonyl)imide anion.[39] Recently they also reported the temperature dependence of the low-frequency Kerr spectrum for the RTIL 1-pentyl-3-methylimidazolium bis(trifluoromethylsulfonyl)imide.[40] Giraud *et al.* studied five typical imidazolium ionic liquids.[41] They analyzed the low-frequency Kerr spectra of the ionic liquids using a multimode Brownian oscillator model and concluded that the signals from each of the five ionic liquids are dominated by the imidazolium cation dynamics. Cang, Li, and Fayer studied the dynamics of the RTIL 1-ethyl-3-methylimidazolium nitrate and concentrated on diffusive relaxation processes with the time range from 1 ps to 2 ns.[42] They described the temperature dependence of the observed diffusive relaxation decays using a mode-coupling theory for the dynamics, in which the data are fit to a function where a sum of two power-law decays describes the faster relaxation processes, and this sum is multiplied by a slower exponential decay assigned to the α relaxation.

In this paper, we present high quality Kerr transient data for each of the five pyrrolidinium RTILs shown in Fig. 1. There are several reasons for investigating nonaromatic ionic liquids. The electronic structure of the aromatic molecular cations is more delocalized than for the aliphatic molecular cations leading to ion-ion interactions of a different nature. In a number of cases, cyclic aromatic molecules are more toxic than molecules with the corresponding aliphatic ring systems. If this proves true for RTILs, then the aliphatic cation RTILs might be better choices from an environmental perspective. We have studied the following five different pyrrolidinium ionic liquids shown in Fig. 1: *N*-butyl-*N*-methylpyrrolidinium bis(trifluoromethylsulfonyl)imide (P_{14}^{+}/NTf_2^{-}), *N*-methoxyethyl-*N*-methylpyrrolidinium bis(trifluoromethylsulfonyl)imide (P_{1EOM}^{+}/NTf_2^{-}), *N*-ethoxyethyl-*N*-methylpyrrolidinium bis(trifluoromethylsulfonyl)imide (P_{1EOE}^{+}/NTf_2^{-}), *N*-ethoxyethyl-*N*-methylpyrrolidinium bromide (P_{1EOE}^{+}/Br^{-}), and *N*-ethoxy-ethyl-*N*-methyl-pyrrolidinium dicyanoamide (P_{1EOE}^{+}/DCA^{-}). We will compare the dynamical aspects of the cations using measurements from the series of NTf_2^{-} anion RTILs of P_{14}^{+}/NTf_2^{-}, P_{1EOM}^{+}/NTf_2^{-}, and P_{1EOE}^{+}/NTf_2^{-}. The effects on liquid dynamics from anion motions are investigated by comparing dynamics from P_{1EOE}^{+}/NTf_2^{-}, P_{1EOE}^{+}/Br^{-}, and P_{1EOE}^{+}/DCA^{-}. For the case of P_{1EOE}^{+}/Br^{-}, we can measure cation dynamics directly because the spherical bromide anion cannot directly contribute to the OHD-RIKES signal, since this signal depends on fluctuations of the polarizability anisotropy.

II. EXPERIMENT

A. Sample preparation

The synthesis of the ionic liquids used in this study will be reported in detail elsewhere,[43] so only a brief description of the procedures used are presented here. The pyrrolidinium cations were synthesized via standard methods, viz. quaternization of *N*-methylpyrrolidine with the appropriate alkyl halide (in this case bromide) to produce the pyrrolidinium bromide salts.[44–46] These were metathesized to the bis(trifluoromethylsulfonyl)imide salt using equimolar quantities of the pyrrolidinium bromide and lithium bis(trifluoromethylsulfonyl)imide in aqueous solution.[45,47] Metathesis of the pyrrolidinium bromide to the dicyanoamide salt was done according to Refs. 47 and 48 by reacting equimolar quantities of silver dicyanoamide[48] with the appropriate pyrrolidinium bromide in water, filtering off the silver bromide precipitate, and evaporating off the aqueous phase. The pyrrolidinium dicyanoamide was extracted from the residue into dichloromethane, which was filtered and evaporated to yield the pure ionic liquid.[48,49] The resultant liquids were decolorized by stirring with activated charcoal overnight and then passing a solution of the liquid in acetonitrile through an activated alumina column. All ionic liquids were dried at reduced pressure at 318 K for more than 24 h prior to characterization and use. All starting materials were purchased from Aldrich in the highest available purity grade and used as received. Viscosity measurements were made using a temperature-controlled Cambridge Applied Systems reciprocating electromagnetic piston viscometer (ViscoLab 4100). No impurity signals were detected in the ^{1}H-NMR spectra of the neat ionic liquids.

B. OHD-RIKES measurement

Details of the OHD-RIKES apparatus were reported elsewhere.[38,50] Briefly, a lab-built femtosecond titanium sapphire laser operating at 800 nm center wavelength was used as a light source. The output power was about 320 mW when the laser was pumped by 3.2 W of 532 nm light from a frequency-doubled diode-pumped continuous $Nd:VO_4$ laser (Spectra Physics, Millennia V). To compensate for the group velocity dispersion introduced by the optics in the spectrometer, the laser output was first routed through a retroreflecting dispersive delay line consisting of a pair of fused silica Brewster prisms separated by ≈120 cm. After the delay line the laser pulses passed thorough a half-wave plate to rotate their polarization to vertical, and were incident on an uncoated fused silica interferometric wedge to produce pump and probe beams with an intensity ratio of about 90:5. The pump beam is routed though a half-wave plate and a Glan–Thompson polarizer transmitting vertically polarized light prior to the focusing lens. The pump beam intensity was modulated at 1 kHz by a mechanical chopper (Stanford Research Systems, SR540). The probe beam is routed through an antireflection coated interferometer wedge, a variable optical delay line (Pacific Precision Labs, 0.1 micron accuracy), a half-wave plate and a Glan–Thompson polarizer to set the polarization 45° from vertical, and then through a quarter-wave plate before the fused silica focusing lens. The pump and probe beams were focused on the sample and recollimated with a matched pair of 100 mm focal length fused silica lenses. The pump beam was blocked while the probe was sent though a second Glan–Thompson polarizer and a spatial filter consisting of two 150 mm lenses and a 0.15 mm pinhole. To achieve heterodyne detection, an out of phase local oscillator was introduced by rotating the input polarizer by ±1° away from the homodyne orientation (defined at the polarizer extinction angle). The OHD-RIKES probe beam was detected by a large area amplified p-i-n photodiode (New Focus, 2032) and recorded as a function of pump-probe delay by a digital lock-in amplifier (Stanford Research Systems, SR830) referenced to the chopper frequency. The laser pulse cross correlation measured with a 200 μm potassium dihydrogen phosphate crystal was 36±3 fs FWHM (equivalent to a 25±2 fs pulse, assuming a Gaussian line shape). The measured spectral bandwidth of the laser pulses was about 55 nm. All the measurements were made at 295±2 K. Scans with high time resolution of 4096 points at 0.5 μm/step were recorded for a time window of 13.66 ps. The slower orientational dynamics were captured in 115 ps scans with 20 μm per data point and in 730 ps scans with 50 μm per data point. Ten scans were averaged for the short time window transients (5 scans each for +1° and −1° rotations of the probe input polarizer) and 20 scans were averaged for the intermediate and long time windows (10 scans each for both the +1° and −1° rotations of the probe input polarizer).

C. Density functional theory calculations

Optimized geometries, intramolecular vibrational modes, and effective atom-centered charges for the three pyrrolidinium cations P_{1EOE}^+, P_{1EOM}^+, and P_{14}^+, and for the NTf_2^- and DCA^- anions of the ionic liquids were performed by using the GAUSSIAN 03 program package.[51] Becke's three-parameter gradient-corrected exchange[52] and Lee–Yang–Parr gradient-corrected correlation functions[53] (B3LYP) were used with the 6-31+G(d,p) basis set.[51] Calculations were done for the isolated molecular ion and again for the ion in a dielectric continuum model using a dielectric constant of 36.64 for acetonitrile. The value for the acetonitrile dielectric constant was chosen because of the similar solvatochromic effects observed in ionic liquids.[54] The integral equation formalism, polarized continuum model (IEF-PCM) of Mennucci and Tomasi[55,56] was used to mimic a solvent environment similar to that observed for solvatochromic shifts in several ionic liquids. Molecular ion geometries were optimized with no constraints. The *XYZ* Cartesian coordinates for cation and anion optimized by B3LYP/6-31+G(d,p) calculations are summarized in the EPAPS supporting information document.[57]

III. RESULTS

A. Picosecond reorientational dynamics

Figure 2 shows the log-log plots of the Kerr transients of the five pyrrolidinium ionic liquids. As shown in Fig. 2, the Kerr transients of P_{1EOE}^+/NTf_2^-, P_{1EOM}^+/NTf_2^-, and P_{14}^+/NTf_2^- are quite similar. On the other hand, the Kerr transients for P_{1EOE}^+/Br^- and P_{1EOE}^+/DCA^- are clearly distinguishable. The Kerr transient of P_{1EOE}^+/Br^- shows that the amplitude of the picosecond reorientational relaxation is much smaller than that of the other ionic liquids.

In Fig. 2, one finds that for time delays from 10 fs to 1 ps, a strong beating pattern is observed in the Kerr transients. The beats arise from multiple intramolecular normal modes, and are most complex for the RTILs with the NTf_2^- anion. A different beating pattern with a smaller modulation depth is observed over the same time range for the P_{1EOE}^+/Br^- liquid. For the P_{1EOE}^+/DCA^- liquid, the beating pattern is a more simple sinusoidal decay over this time range, indicating the presence of a single dominant low-frequency mode. In the 1 to 10 ps time window, the intramolecular modes are damped. For longer time scales beyond 10 ps, the intramolecular vibrational damping is complete and a nonexponential decay is observed for each of the five liquids.

The overdamped nonexponential decay part of the Kerr transients from 2 to 740 ps is fit to several model functions. Exponential, stretched exponential, biexponential, and a sum of exponential plus stretched exponential functions do not adequately fit the data. Both triexponential and mode coupling theory model functions[42] provide improved quality fits, but a triexponential model is generally superior. We note that the long time noise floor for our Kerr transients ranges between 2×10^{-5} to 5×10^{-5} on an intensity scale normalized to the peak of the electronic response. To obtain a reduced noise floor, it would be necessary to either use a scheme with multiple laser pulses of different durations and intensities as done by the Fayer group,[42] or to employ a multiple modulation method as demonstrated by Fourkas and co-workers.[58] A

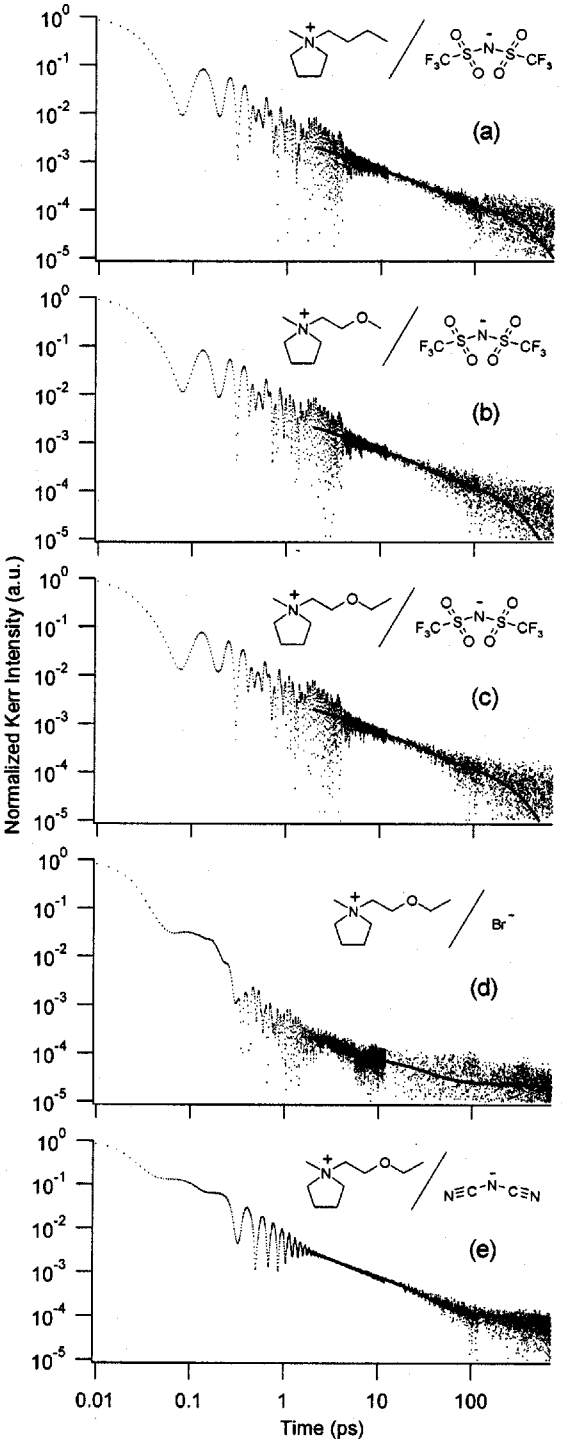

FIG. 2. Log-log plots of Kerr transients for (a) P_{1EOE}^{+}/NTf_2^{-}, (b) P_{1EOM}^{+}/NTf_2^{-}, (c) P_{14}^{+}/NTf_2^{-}, (d) P_{1EOE}^{+}/Br^{-}, and (e) P_{1EOE}^{+}/DCA^{-}. Triexponential fit functions are also shown in the figure.

reduced noise floor will be required to differentiate between the triexponential decay and mode-coupling theory[42] models.

The triexponential fit curves are also shown in Fig. 2. The fit parameters are summarized in Table I and plotted in Fig. 3. The sum of the amplitudes is normalized to unity. The amplitudes of the diffusive relaxation components relative to the instantaneous electronic responses are also listed. The notable points from Table I are the following: (1) the amplitude of the diffusive relaxation for P_{1EOE}^{+}/Br^{-} relative to the electronic contribution is only about 10% of that for the other ionic liquids, (2) the fast and intermediate relaxation time constants τ_1 and τ_2 do not vary much between these five ionic liquids, and (3) the slow relaxation time constants τ_3 for the five pyrrolidinium RTILs range from 160 ps to 3.2 ns, and correlate with the values of the shear viscosity.

B. Femtosecond dynamics: Low-frequency Kerr spectrum

The Kerr transients are analyzed by means of the Fourier transform deconvolution procedure introduced by McMorrow and Lotshaw.[26,27] To obtain a sufficient number of data points for a spectrum of reasonable accuracy, it is necessary to extend the high time resolution data from Fig. 2 (with 4096 data points over the time window from −1.5 to 12 ps) over a longer time range than it is practical to record. To achieve this, the longer time scale Kerr transients (Fig. 2) in the range from 2 to 740 ps were recorded with lower time resolution, and are fit to a triexponential function $(a_1 \exp(-t/\tau_1)+a_2 \exp(-t/\tau_2)+a_3 \exp(-t/\tau_3))$. Prior to Fourier-transform analysis, the 4096 point data set from −1.5 to 12 ps is extended to 131 072 points using the triexponential fit function with a time step of 3.3355 fs, yielding spectra with about 0.0763 cm^{-1}/point spacing. All the spectra obtained in this study are well resolved up to 750 cm^{-1}.

Figure 4 shows the Fourier-transform Kerr spectra of the five ionic liquids. These spectra have had the contribution from the diffusive components subtracted prior to Fourier deconvolution. As shown in Fig. 4, P_{1EOE}^{+}/NTf_2^{-}, P_{1EOM}^{+}/NTf_2^{-}, and P_{14}^{+}/NTf_2^{-} show rich intramolecular vibrational bands spectra in comparison with P_{1EOE}^{+}/Br^{-} and P_{1EOE}^{+}/DCA^{-}. The spectra of P_{1EOE}^{+}/NTf_2^{-}, P_{1EOM}^{+}/NTf_2^{-}, and P_{14}^{+}/NTf_2^{-} are quite similar. The frequencies of the intramolecular vibrational modes observed in the Kerr spectra of the ionic liquids are summarized in Table II. P_{1EOE}^{+} intramolecular vibrational bands are observed at band centers of 283, 380, 527, and 642 cm^{-1} in P_{1EOE}^{+}/Br^{-} and P_{1EOE}^{+}/DCA^{-}, though they are of much lower intensity compared to the strong intramolecular bands of the NTf_2^{-} anion.

C. Density functional theory calculations

The electrostatic properties for each of the five molecular ions are obtained following geometry optimizations. Atom-centered charges from the ChelpG model are obtained for the gas-phase ion, for the PCM model using the gas-phase geometry, and again for a geometry reoptimization for the stable ground state with PCM polarization. The magnitudes of the atom-centered charges are enhanced relative to the gas phase when the IEF-PCM model is applied, and are further enhanced as the geometry is reoptimized from the gas phase. The electric multipole moments obtained are for the standard orientation, center-of-mass coordinate system. It is important to note that dipole moments for ions depend on the choice of origin for the atomic coordinates. Optimized ge-

TABLE I. Triexponential fit parameters for diffusive Kerr transients of pyrrolidinium ionic liquids.

Ionic liquid	a_{od}[a]	a_1[b]	τ_1(ps)[c]	a_2[d]	τ_2 (ps)[d]	a_3[d]	τ_3(ps)[e]
P_{1EOE}^+/NTf_2^-	3.52×10^{-3}	0.71	2.31	0.23	15.4	0.06	165
P_{1EOM}^+/NTf_2^-	3.63×10^{-3}	0.68	2.27	0.26	14.6	0.06	161
P_{14}^+/NTf_2^-	3.41×10^{-3}	0.72	2.43	0.22	18.3	0.06	253
P_{1EOE}^+/Br^-	0.47×10^{-3}	0.78	1.89	0.17	21.2	0.05[f]	3200[g]
P_{1EOE}^+/DCA^-	5.66×10^{-3}	0.78	2.02	0.20	16.2	0.02	686

[a]Sum of amplitudes of triexponential function normalized by the instantaneous electronic Kerr response.
[b]Error is ±10%.
[c]Error is ±20%.
[d]Error is ±30%.
[e]Error is ±35%.
[f]Error is ±50%.
[g]Error is ±100%.

ometry coordinates, rotational constants, CHelpG charges, and electrostatic properties are reported in the supporting information.[57]

Harmonic frequencies for each of the optimized geometries were calculated, both for the isolated gas-phase molecular ion, and with the polarized continuum model using the value for the room temperature dielectric constant of acetonitrile. The complex vibrational spectroscopy resulting from the flexibility of each ion makes most comparisons of observed versus calculated modes difficult. An exception is the pentaatomic dicyanoamide anion, which has a strong bending mode observed at 180 cm^{-1} for which calculated values are 160 cm^{-1} (gas phase) and 174 cm^{-1} (PCM optimized); and the symmetric in-plane cyano wagging mode observed experimentally at 663 cm^{-1} and calculated to be at 650 cm^{-1} for the PCM model.

IV. DISCUSSION

Reorientational relaxation signals from optical Kerr effect experiments provide a measure of the collective response τ_{col}, unlike single particle experiments, such as NMR relaxation. The collective reorientational relaxation time τ_{col} is correlated with the single molecule reorientation time τ_{rot},[59]

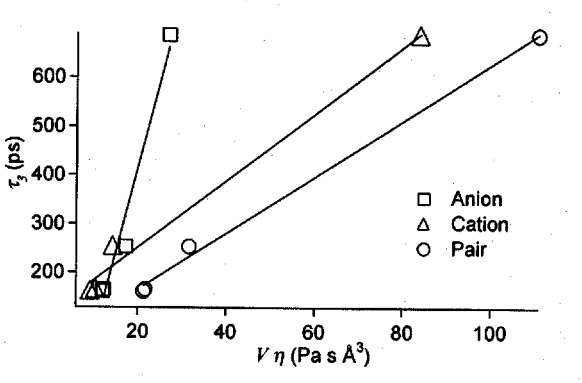

FIG. 3. Plots of the slow relaxation time constant τ_3 vs ηV for the five pyrrolidinium ionic liquids. Squares, triangles, and circles represent points calculated using the molecular volumes of the anion, cation, and the sum of cation and anion, respectively.

$$\tau_{col} = \frac{g_2}{j_2}\tau_{rot}, \tag{1}$$

where g_2 is the static pair orientational correlation parameter and j_2 is the dynamical orientational correlation pair parameter.[59] Although it is difficult to estimate g_2 and j_2 for the RTIL molecular ions, the collective (structural) reorientational time is proportional to the single molecule reorientational time if the ratio of g_2 to j_2 does not vary between the five pyrrolidinium RTILs. Comparisons between NMR and neutron scattering experiments and molecular dynamics simulations will be required to address the characteristics of g_2 and j_2 for ionic liquids.

Results from the triexponential analysis of the longer time Kerr transients are summarized in Table I. Only the longest time constant τ_3 varies with viscosity in a manner consistent with diffusive relaxation. For diffusive orientational relaxation, the reorientation time constant τ_{rot} of a solute in many simple organic molecular liquids is well described by the Stokes–Einstein–Debye hydrodynamic model,[60]

$$\tau_{rot}^L = \frac{6V\eta f}{L(L+1)k_BT}, \tag{2}$$

where V is the volume of the rotating species, η is the shear viscosity of the liquid, f is a shape factor, k_B is the Boltzmann constant, T is the absolute temperature, and the rank L equals 2 for depolarized Kerr reorientation signals. Figure 3 shows the plots of the longest reorientation time τ_3 versus V_η for the pyrrolidinium ionic liquids. Because the fitted time constant τ_3 for P_{1EOE}^+/Br^- is 3.2 ns, which is more than four times longer than the time window for the present OHD-RIKES measurements, only the τ_3 values for P_{14}^+/NTf_2^-, P_{1EOM}^+/NTf_2^-, P_{1EOE}^+/NTf_2^-, and P_{1EOE}^+/DCA^- are plotted in Fig. 3. The values for several physical properties including formula weight M_W, density d, formula volume V, viscosity η of the pyrrolidinium RTILs are summarized in Table III. The values of V for the ionic liquid cations and anions are estimated by the method of van der Waals increments,[61,62] with the value of V for the Br^- ion taken from Israelachvili's book.[63]

Figure 3 plots the longest Kerr relaxation time constant τ_3 versus the product of the shear viscosity times the volume

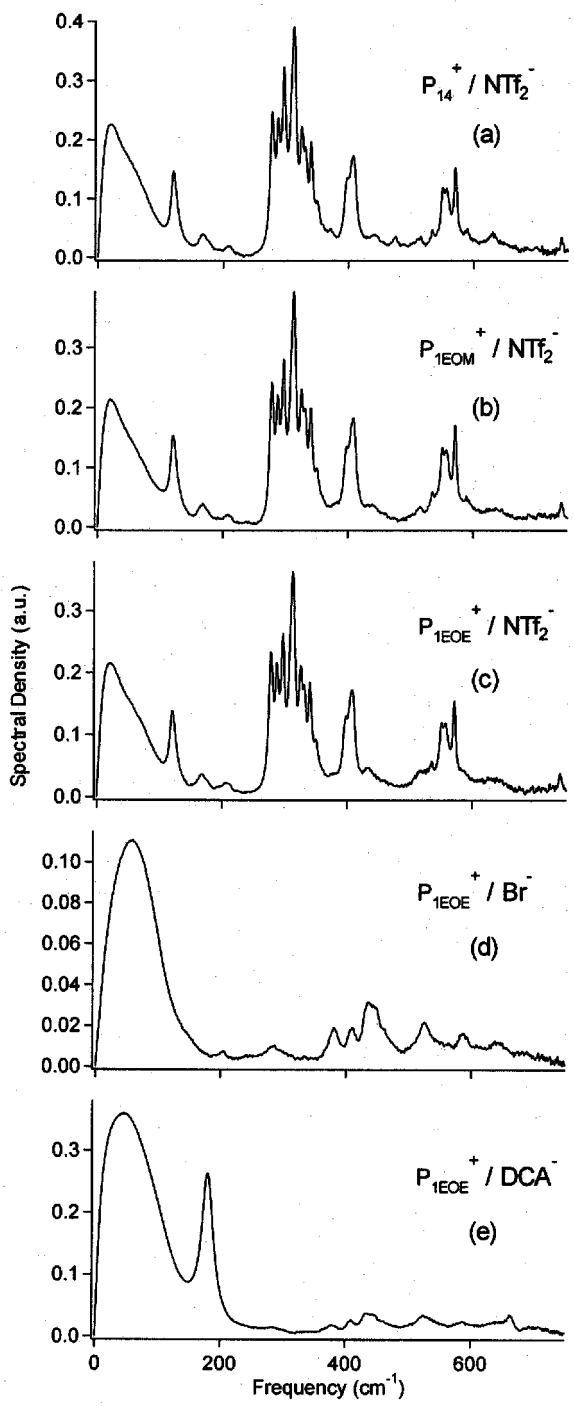

FIG. 4. Fourier-transform frequency power spectra of (a) P_{1EOE}^+/NTf_2^-, (b) P_{1EOM}^+/NTf_2^-, (c) P_{14}^+/NTf_2^-, (d) P_{1EOE}^+/Br^-, and (e) P_{1EOE}^+/DCA^-. The contribution of the picosecond relaxation was subtracted.

for each of the pyrrolidinium RTILs, excepting P_{1EOE}^+/Br^-. Using either the cation or anion volume to calculate the graph abscissa, a rough correlation is observed. However, noticeably better agreement and a better statistical linear correlation are found when the volume is taken to be the sum of the cation plus anion molecular volumes, $V_{total}=V_{cation}+V_{anion}$. If the slowest orientational relaxation process observed in the Kerr signal (characterized by the time constant τ_3) arises from predominantly cation or anion reorientation, one expects to find a linear relationship between τ_3 and either of the viscosity-volume products $V_{anion}\eta$ or $V_{cation}\eta$. In a recent molecular dynamics study of solvation in the RTIL 1-butyl-3-methylimidazolium hexafluorophosphate, Kobrak and Znamenskiy found that the dynamics of anions and cations are strongly coupled.[64] Margulis also showed the strong correlation between cation and anion diffusions in 1-alkyl-3-methylimidazolium hexafluorophosphate ionic liquids by molecular dynamics simulation.[65] Thus, we believe it is plausible that the Kerr orientational signal is comprised of a sum of orientational correlations of individual cations and anions, as well as cation-anion pairs. We cannot exclude the possibility that there is a contribution to the overall diffusive response from more complex transient aggregates, such as cation-anion-cation or anion-cation-anion trimers. To contribute to the Kerr diffusive reorientation signal, such aggregates would have to have a cluster lifetime greater than the jump diffusion time.

Cang, Li, and Fayer measured the Kerr relaxation dynamics of 1-ethyl-3-methylimidazolium nitrate at the temperature range of 295–410 K.[42] They found that the relaxation was best fit to a model from mode coupling theory. This model is the product of the sum of two power-law decays multiplied by a slower exponential decay, which is assigned to the overall α relaxation of the glassy liquid.[42] Their results showed that the longest α-relaxation time constant follows the trend predicted by the Stokes–Einstein–Debye hydrodynamic model if the rotating solute volume is taken as the volume of only the cation. In the pyrrolidinium RTILs, it is possible that the appropriate volume of a rotor may be that of the sum of the cation and anion volumes. Temperature dependent Kerr dynamics experiments of both nonspherical anion and cation ionic liquids will be needed to obtain further understanding of reorientation dynamics in room temperature ionic liquids. To study whether clustering affects the measured reorientation, it will also be helpful to have independent experimental data from NMR and quasielastic neutron scattering. In particular, temperature-dependent NMR experiments will elucidate to what degree internal torsions occur on competing time scales with overall diffusive tumbling motions of the molecular ions.

The values of the fast and intermediate relaxation time constants τ_1 and τ_2 do not vary much between the five pyrrolidinium ionic liquids and have values of about 2 ps and 17 ps, respectively. The corresponding normalized amplitudes for a_1 and a_2 are about 0.73 and 0.22, respectively. Several groups have characterized the solvation dynamics in ionic liquids by time dependent fluorescence Stokes shift measurements of solvatochromic probes such as coumarin 153 and 4-aminopthalimide.[54,66–71] The solvation dynamics show strongly nonexponential relaxation, fitting well to a stretched exponential function with a β value of 0.4–0.5, for both aromatic and nonaromatic RTILs. The average solvation time constants observed in these experiments are substantially longer than the observed Kerr reorientation dynamics, typically occurring on subnanosecond to nanosecond time scales. We have measured solvation dynamics for the pyrrolidinium-cation RTILs P_{14}^+/NTf_2^- and P_{1EOE}^+/NTf_2^-. Preliminary analysis shows that the average relaxation time constant

TABLE II. Intramolecular vibrational band frequencies observed in Fourier-transform Kerr spectra of ionic liquids. In the Assignment column, *A* denotes an anion vibration and *C* a cation vibration.

$P_{14}^+/NTf_2^-(cm^{-1})$	$P_{1EOM}^+/NTf_2^-(cm^{-1})$	$P_{1EOE}^+/NTf_2^-(cm^{-1})$	$P_{1EOE}^+/Br^-(cm^{-1})$	$P_{1EOE}^+/DCA^-(cm^{-1})$	Assignment
121	121	121			*A*
168	168	168			*A*
				180	*A*
			203		*C*
208	208	208			*A*
278	278	278			*A*
			284	282	*C*
288	288	288			*A*
297	297	297			*A*
313	313	313			*A*
326	326	326			*A*
331	331	332			*A*
340	341	341			*A*
350	350	350			*A*
371					*C*
			381	380	*C*
399	398	399			*A*
407	408	408			*A*
			410	411	*C*
440	435	433	440	439	*C*
475					*C*
			526	528	*C*
534	535	535			*A*
551	551	551			*A*
557	557	557			*A*
571	571	571			*A*
588	589	587	587	587	*C*
630					*C*
			641	643	*C*
				663	*A*
740	741	740			*A*

TABLE III. Formula weight M_W, density d, formula volume V, and viscosity η of the five pyrrolidinium ionic liquids.

Ionic liquid	Constituent	M_W(g/mol)	d^a(g/cm^3)	V^b(Å^3)	η^c(cP)
P_{1EOE}^+/NTf_2^-		438.4	1.41	378	60
	P_{1EOE}^+	158.3		175	
	NTf_2^-	280.1		203	
P_{1EOM}^+/NTf_2^-		424.4	1.46	361	59
	P_{1EOM}^+	144.3		158	
	NTf_2^-	280.1		203	
P_{14}^+/NTf_2^-		422.4	1.40	372	85
	P_{14}^+	142.3		169	
	NTf_2^-	280.1		203	
P_{1EOE}^+/Br^-		238.2	1.31	206	11 940
	P_{1EOE}^+	158.3		175	
	Br^-	79.9		31	
P_{1EOE}^+/DCA^-		219.8	1.10	231	480
	P_{1EOE}^+	158.3		175	
	DCA^-	66.0		56	

[a]Values at 295 K.
[b]Estimated by van der Waals increments (Refs. 61 and 62).
[c]Values at 296 K.

from fluorescence Stokes shift measurements seems to be substantially slower than the slowest observed Kerr relaxation time constant τ_3.

The bands observed in the P_{1EOE}^+/Br^- spectrum are assigned to the intramolecular vibrational bands of the P_{1EOE}^+ cation because the monatomic Br^- ion has no vibrational modes. Comparing the spectra of P_{1EOE}^+/Br^- and P_{1EOE}^+/DCA^-, we find that P_{1EOE}^+/DCA^- shows a strong vibrational mode at 180 cm^{-1}. Lower intensity intramolecular modes for P_{1EOE}^+/DCA^- are observed in the 200–750 cm^{-1} range and are quite similar to those of P_{1EOE}^+/Br^-, except for the 663 cm^{-1} band which is present only in P_{1EOE}^+/DCA^-. The normal modes calculated at the B3LYP/6-31+G(d,p) level, listed in Table II, show that the 180 cm^{-1} DCA^- band is the cyano-*N*-cyano bending mode and the 663 cm^{-1} band is the *N*-cyano bending mode.

The ionic liquids having the NTf_2^- anion display a rich vibrational structure, as seen in Fig. 4. The intramolecular vibrational bands of the NTf_2^- anion dominate the spectra of P_{1EOE}^+/NTf_2^-, P_{1EOM}^+/NTf_2^-, and P_{14}^+/NTf_2^- because the NTf_2^- anion contribution to the Raman spectral density is more than an order of magnitude greater than from the pyrrolidinium cations. For each of the pyrrolidinium NTf_2^- ionic liquid spectra, there are ten intense vibrational transitions in the 250–420 cm^{-1} frequency range (Table II). An electronic structure calculation at the B3LYP/6-31G+(d,p) level for a gas-phase C_2 (trans) symmetry NTf_2^- anion shows only eight intramolecular vibrational bands in the corresponding frequency range. The inconsistency between the number of bands observed in the experimental liquid spectra and the density functional theory normal mode calculations likely arises because the flexible NTf_2^- anion has multiple conformations that lead to shifts in some of the vibrational bands. We note that the Kerr spectra of imidazolium ionic liquids with the NTf_2^- anion also show ten strong vibrational modes in the same frequency region,[41] in common with the pyrrolidinium NTf_2^- ionic liquid spectra presented here. Holbrey, Reichert, and Rogers have reported crystal structures of alkylimidazolium salts, with the NTf_2^- anion having the *cis* conformation.[72] We find overall agreement with the anion and cation vibrational spectra with the Raman spectra of P_{13}^+/NTf_2^- and P_{13}^+/I^- reported recently by Castriota *et al.*[73] and with the IR and Raman spectra of NTf_2^- reported by Rey *et al.*[74]

In order to emphasize the intermolecular vibrational dynamics, Fig. 6 shows the Kerr spectra from Fig. 4 plotted over a narrower spectral window of 0–200 cm^{-1}. The low-frequency dynamics arise from several types of intermolecular interactions including collision-induced and dipole-induced motions with the dominant contributions likely arising from intermolecular librational motions. As shown in Figs. 5 and 6, the broad low-frequency spectra of the P_{1EOE}^+/NTf_2^-, P_{1EOM}^+/NTf_2^-, and P_{14}^+/NTf_2^- liquids are quite similar. However, the low-frequency spectra of P_{1EOE}^+/Br^- and P_{1EOE}^+/DCA^- are quite distinct. The intermolecular dynamics and interactions between NTf_2^- and the three pyrrolidinium cations lead to similar spectra because of the structural and dynamical similarities of the P_{1EOE}^+, P_{1EOM}^+, and P_{14}^+ cations.

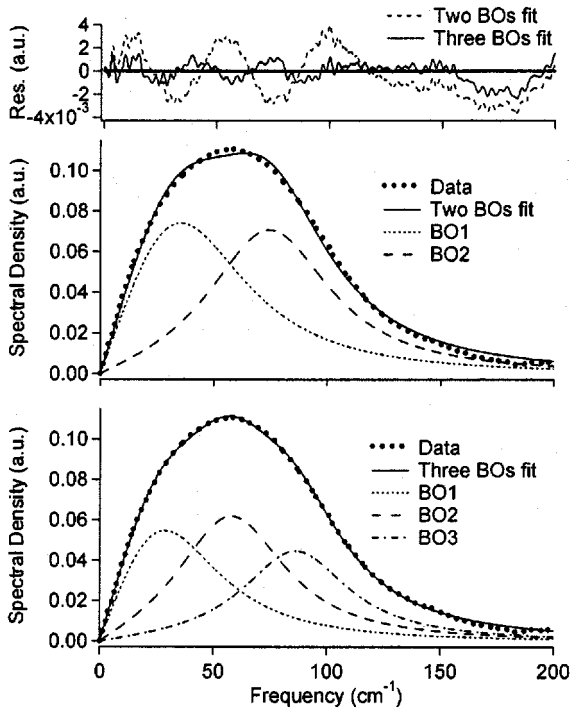

FIG. 5. Multimode Brownian oscillator fits to the intermolecular spectrum of P_{1EOE}^+/Br^- from 0 to 200 cm^{-1}. The bottom figure presents the best fit using three Brownian oscillators, the middle figure the best fit with two Brownian oscillators, and the residuals for both fits are shown at top.

One of the primary challenges in the interpretation of low-frequency Kerr spectra is to fully understand the intermediate time scale dynamics bridging the intermolecular vibrational to diffusive time scales. In a pure liquid, the progression of time scales in the observed dynamics begins at the shortest time scales with the intramolecular vibrations, followed by underdamped intermolecular vibrations (including librational motions), with the longer time scales comprised of a quasiexponential decay for the intermediate time dynamics, with the longest time scale relaxation being represented in the simplest case by a single exponential decay that is correlated with diffusive reorientational motions. Detailed tests of the models have been made for two different cases. Loughnane *et al.* showed that the intermediate time scale exponential decay can be described as resulting from motional narrowing of intermolecular oscillators.[75] They showed that this explanation was consistent for six symmetric top liquids for a wide variety of temperatures. On the other hand, McMorrow *et al.* showed that a single "quantum" harmonic oscillator reproduces the dynamics of CS_2 over a range of dilution concentrations for which the chemical environment changes substantially (as evidenced by the change in observed linewidth).[76,77] The quantum harmonic oscillator has the advantage that the dephasing rate is not coupled to the frequency of the oscillator. A limitation of the "classical" harmonic oscillator model is that it exhibits *frequency pulling*, and hence distortions of the lineshapes because of the strong overlap between inhomogeneous spectral widths and dynamical time scales. For the room temperature ionic liquids discussed here, the low-frequency spectra mea-

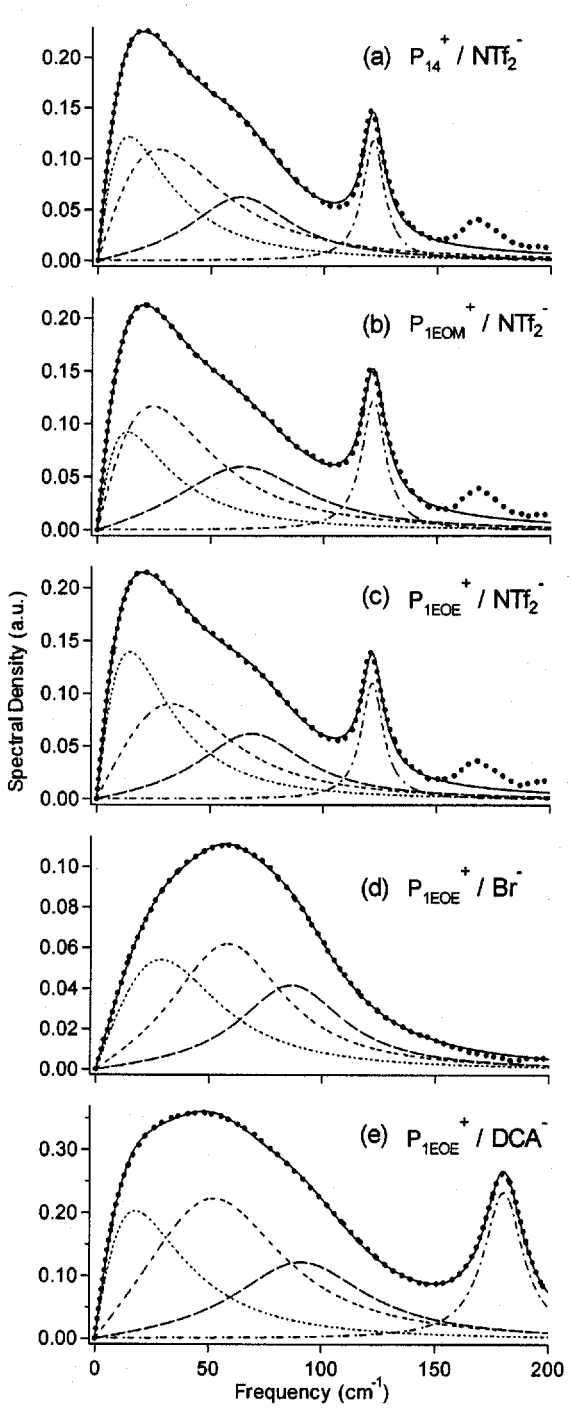

FIG. 6. Low-frequency power spectra of (a) P_{1EOE}^+/NTf_2^-, (b) P_{1EOM}^+/NTf_2^-, (c) P_{14}^+/NTf_2^-, (d) P_{1EOE}^+/Br^-, and (e) P_{1EOE}^+/DCA^- (bold dotted lines). Entire fit curves (solid lines) and each Brownian oscillator fits (small dotted, short dashed, and long dashed lines) are also shown. Intramolecular modes are also fitted by a Lorentzian function (dot-dash lines).

sured in the 0–150 cm^{-1} range arise from intermolecular dynamics from both the cations and anions. The complexity of the observed ionic liquid spectra does not permit us to distinguish between the motional narrowing or quantum harmonic oscillator models in the Kerr dynamics observed for the pyrrolidinium RTILs.

The low-frequency intermolecular dynamics in the pyrrolidinium RTILs are analyzed by line shape fitting of the broad spectral band to a multimode Brownian oscillator model,[78,79]

$$I_{BOi}(\omega) = \sum_{i=1}^{3} \frac{a_{BOi}\omega}{2\pi[(\omega_{BOi}{}^2 - \omega^2)^2 + \gamma_{BOi}{}^2\omega^2]}, \tag{3}$$

where a_{BOi}, ω_{BOi}, and γ_{BOi} are the amplitude, the frequency, and the damping parameters for the ith Brownian oscillator, respectively. Though the linewidth coefficient γ_{BOi} was originally assumed to be frequency dependent,[78,79] here it is assumed to be constant for simplicity. Fits to the intermolecular spectral bands using two-mode versus three-mode Brownian oscillators are shown in Fig. 5 for P_{1EOE}^+/Br^-. For the two-mode model, the fit curve deviates somewhat from the data and the fit residuals are noticeably worse than for the three-mode model for which we determined that adequate fits were obtained. We note that even small molecular liquids normally show at least two features in fits to the intermolecular Kerr spectrum. For the more complex ionic liquid case, it is plausible that even more than three modes could be present, likely with substantial overlap between modes. At least three Brownian oscillators are needed to obtain good fits to the intermolecular dynamics of the pyrrolidinium RTILs. We note that Giraud *et al.* used three Brownian oscillators to describe the intermolecular Kerr spectra of five imidazolium cation ionic liquids.[41] A Lorentzian function is added to the model to account for the intramolecular bands observed at 180 cm^{-1} for P_{1EOE}^+/DCA^- and at 122 cm^{-1} for P_{1EOE}^+/NTf_2^-, P_{1EOM}^+/NTf_2^-, and P_{14}^+/NTf_2^-. Figures 5 and 6 show the low-frequency spectra and Brownian oscillator fits. The fit parameters are summarized in Table IV. The sum of the spectral area $A_{BOi}=\int I_{BOi}(\omega)d\omega/\Sigma_i\int I_{BOi}(\omega)d\omega$ for the Brownian oscillators is normalized to unity.

From the line shape analysis of the three NTf_2^- anion RTILs shown in Fig. 6, one finds that the band center frequencies ω_{BOi} of about 28, 45, and 72 cm^{-1} are very similar for P_{14}^+/NTf_2^-, P_{1EOM}^+/NTf_2^- and P_{1EOE}^+/NTf_2^-. The P_{1EOE}^+/Br^- intermolecular spectrum arises predominantly from P_{1EOE}^+ cation dynamics, because the spherical bromide ion has no reorientational contribution to the depolarized OHD-RIKES signal. Three Brownian oscillator components centered at 43, 66, and 91 cm^{-1} are found in the P_{1EOE}^+/Br^- spectrum, with the band center for the intermolecular spectrum shifted to higher frequency, as observed in Fig. 6. Intermolecular dynamics for P_{1EOE}^+/DCA^- liquids also show a higher frequency first moment of the spectrum. Brownian oscillator line shape components are fit to the center frequencies of 34, 64, and 97 cm^{-1}. We note that the reduced mass between cation and anion for the NTf_2^- liquids is approximately two times greater than for either of the P_{1EOE}^+/Br^- or P_{1EOE}^+/DCA^- liquids. Thus a spectral component arising from a vibrational coordinate between cation and anion could account for the observed higher band center frequencies for the latter two liquids.

For the five pyrrolidinium ionic liquids considered here, the case of the intermolecular vibrations is simplest to consider for P_{1EOE}^+/Br^- because of the spherical bromide anion.

TABLE IV. Brownian oscillator fit parameters for the low-frequency power spectra of the pyrrolidinium ionic liquids.

Ionic liquid	A_{BO1}[a]	$\omega_{BO1}(cm^{-1})$[b]	$\gamma_{BO1}(cm^{-1})$[c]	A_{BO2}[b]	$\omega_{BO2}(cm^{-1})$[d]	$\gamma_{BO2}(cm^{-1})$[d]	A_{BO3}[b]	$\omega_{BO3}(cm^{-1})$[d]	$\gamma_{BO3}(cm^{-1})$[d]
P_{1EOE}^{+}/NTf_2^{-}	0.23	28	61	0.44	47	76	0.33	74	65
P_{1EOM}^{+}/NTf_2^{-}	0.17	29	71	0.45	41	81	0.38	73	73
P_{14}^{+}/NTf_2^{-}	0.21	28	68	0.55	45	86	0.24	69	61
P_{1EOE}^{+}/Br^{-}	0.27	43	72	0.40	66	62	0.32	91	57
P_{1EOE}^{+}/DCA^{-}	0.17	34	76	0.48	64	79	0.35	97	72

[a]Error is ±30%.
[b]Error is ±15%.
[c]Error is ±20%.
[d]Error is ±10%.

The only way in which the Br^{-} motions can couple to the observed Kerr signal is if P_{1EOE}^{+}/Br^{-} interactions lead to substantial changes to the P_{1EOE}^{+} angular momentum. The complex nature of ion-ion structure and interactions in ionic liquids leads us to consider the possibility that low-frequency cation-anion modes may contribute to the intermolecular spectrum along with librations and interaction-induced motions. Visualization of the normal modes for AM1 gas-phase semiempirical cluster calculations on the P_{1EOE}^{+}/Br^{-} dimer and the $Br^{-}/P_{1EOE}^{+}/Br^{-}$ trimer gave preliminary evidence that several of the numerous low-frequency torsional modes of the cation are strongly coupled to bromide translations, leading to effective cation-anion stretching coordinates.

Several line shape models have been used to analyze the low-frequency intermolecular part of OHD-RIKES spectrum for molecular liquids.[33,34,38,50,80–91] The low-frequency intermolecular spectrum of liquids contains the interaction-induced (translational) and librational (reorientational) motions.[92–96] The recent study by Ryu and Stratt on the intermolecular dynamics and calculated Kerr spectra of benzene and CS_2 liquids provides insight for how we may consider ionic liquids in a way that goes beyond line shape analyses.[96] They demonstrated that significant overlap occurs between translational and orientational components of the calculated Kerr low-frequency spectrum in the range from 0 to 200 cm^{-1}. We believe that similar overlap and coupling between translational and orientational modes will also occur for ionic liquids in general. Our geometry optimized gas-phase structures for the three pyrrolidinium cations and two molecular anions show that each ion is an asymmetric rotor. Structures of these ions are actually surprisingly close to symmetric rotors, showing a crude similarity to the rotational symmetry of benzene in the sense that they have two very similar inertial axes for the prolate rotors. In order to unravel the complex intermolecular spectrum in a binary system such as an ionic liquid, we must recognize that there will be low-frequency interaction-induced contributions from both cation and anion, as well as cross terms. Because of the near symmetric top nature for both the cation and anion geometries, there will exist librational motions on two different time scales. Because of the asymmetric nature of the ions, we expect depolarized contributions from all modes. We believe that the strong electrostatic interactions between ions will lead to a substantially higher degree of clustering for ionic liquids compared to neutral organic liquids. The specific attractive associations between cations and anions will lead to vibrational coordinates that should result in more clearly defined modes than are observed for the intermolecular interactions found between aprotic organic liquid molecules. These proposed vibrational coordinates between cations and anions would likely overlap with both the translational (interaction-induced) and orientational (librational) components of the Kerr spectrum. It seems clear that careful molecular dynamics simulations followed by calculation of the Kerr spectra will be required to obtain any more definitive assignments of the low-frequency spectra of ionic liquids. Our conclusion is that the clearest contributions from a line shape analysis are that one obtains an accurate parametrization of the line shape and a reasonably good picture about the minimum number of different modes that contribute to the intermolecular line shape.

The intermolecular dynamics for the five pyrrolidinium RTILs studied here are qualitatively similar to those observed for the imidazolium cation based RTILs studied by Giraud *et al.*[41] and Rajian *et al.*[40] Despite the qualitative similarity in intermolecular dynamics for the two classes of RTILs, the solvent reorganization dynamics probed using solvatochromic fluorescent dyes very different. For each of the imidazolium-cation RTILs investigated thus far, the solvation dynamics present an ultrafast decay component that is qualitatively assigned to librational motions of the aromatic imidazolium cation. Solvation dynamics of RTILs having the same anions but with the aromatic cation replaced by an aliphatic tetraalkylammonium, dialkylpyrrolidinium, or tetraalkylphosphonium cation show slower, glassylike relaxation with long time scale solvation time constants in the range from 50 ps to 50 ns.[54,66–71,97]

It is well known that the dipole moment for an ion is not a very meaningful quantity, since its magnitude depends on the choice of origin for the atomic coordinates. Wynne and co-workers avoid this difficulty by estimating cation effective dipole moments from chemically and structurally similar neutrals.[41] Kobrak has described the how the concept of a "charge arm" can be used in place of the dipole moment for describing polarity in ionic liquids.[98] The charge arm is defined as the charge times distance separating the center of charge and the center of mass. This picture may qualitatively explain the similarity of low-frequency dynamics between NTf_2^{-} ionic liquids with P_{14}^{+} and the aromatic analog 1-butyl-3-methylimidazolium cations because the charge-arms for P_{14}^{+} and 1-butyl-3-methylimidazolium cation have similar values of 0.9 and 1.0 *e* Å, respectively.[98]

Much progress has been made in understanding the properties of room temperature ionic liquids using molecular dynamics simulations. To date, only dialkylimidazolium-cation liquids have been studied. Nonpolarizable potential force fields have been developed using both CHARMM[99] and AMBER[100,101] models, with one work reporting enhanced accuracy by use of a polarizable potential.[102] Fundamental physical properties can be effectively studied with molecular dynamics simulations,[99–101,103,104] as well as solvation energies[105–108] and dynamics.[64,65,109] It will be quite beneficial to compare experiments and theory for optical Kerr dynamics in ionic liquids, as well as to parametrize standard potentials for both nonpolarizable and polarizable potentials for nonaromatic cations and anions such as pyrrolidiniums and NTf_2^-.

V. CONCLUSIONS

The ultrafast dynamical aspects of the five pyrrolidinium ionic liquids have been investigated using femtosecond optical-heterodyne-detected Kerr effect spectroscopy. The picosecond relaxation processes of the five pyrrolidinium ionic liquids show nonexponential behavior, with the best fits obtained using a triexponential model. The fast and intermediate relaxation time constants are about 2 and 20 ps and are almost same for each of the five ionic liquids. The slow relaxation time constant for the ionic liquids correlates with the product of the shear viscosity times the sum of anion and cation volumes, so is roughly consistent with the Stokes–Einstein–Debye hydrodynamic model for orientational friction. The observed viscosities of the pyrrolidinium NTf_2^- and DCA^- ionic liquids indicate that these fluids are well above the glass transition at ambient temperatures. It appears that simple hydrodynamic scaling may be sufficient to explain the faster reorientation of P_{1EOE}^+/NTf_2^- and P_{1EOM}^+/NTf_2^- relative to P_{14}^+/NTf_2^- because of the relative differences in viscosity.

The Fourier-transform Kerr spectra of the five pyrrolidinium ionic liquids have also been obtained. The spectra of the ionic liquids with the NTf_2^- anion (P_{1EOE}^+/NTf_2^-, P_{1EOM}^+/NTf_2^-, and P_{14}^+/NTf_2^-) are quite similar. The intramolecular vibrational bands of P_{1EOE}^+/Br^- and P_{1EOE}^+/DCA^- are similar except for the addition of the DCA^- bending modes. The broad intermolecular spectra of the ionic liquids have been analyzed by the multimode Brownian oscillator model. The intermolecular spectral densities of P_{1EOE}^+/NTf_2^-, P_{1EOM}^+/NTf_2^-, and P_{14}^+/NTf_2^- show maxima at lower frequencies than those of P_{1EOE}^+/Br^- and P_{1EOE}^+/DCA^-. A sum of three Brownian oscillators provides a good fit to the intermolecular line shapes for each of the five ionic liquids studied, though we note that this model may underestimate the complexity of the interactions occurring in such a binary ionic system.

ACKNOWLEDGMENTS

Work done at Rutgers was supported by the National Science Foundation (Grant No. CHE-0239390). Part of this work was carried out at Brookhaven National Laboratory under Contract No. DE-AC02-98CH10886 with the U.S. Department of Energy and supported by its Division of Chemical Sciences, Office of Basic Energy Sciences. Support from the BNL LDRD Program (Project No. 03-118) is acknowledged. The authors thank Mark Kobrak, Elina Trofimovsky, and Kimberly Odynocki for helpful discussions and assistance in the preparation of the ionic liquids.

[1] S. A. Forsyth, J. M. Pringle, and D. R. MacFarlane, Aust. J. Chem. **57**, 113 (2004).
[2] T. Welton, Chem. Rev. (Washington, D.C.) **99**, 2071 (1999).
[3] M. J. Earle and K. R. Seddon, Pure Appl. Chem. **72**, 1398 (2000).
[4] P. Wasserscheid and W. Keim, Angew. Chem., Int. Ed. **39**, 3772 (2000).
[5] T. Kitazume, J. Fluorine Chem. **105**, 265 (2000).
[6] G. W. V. Cave, C. L. Raston, and J. L. Scott, Chem. Commun. (Cambridge) **2001**, 2159.
[7] J. Dupont, R. F. de Souza, and P. A. Z. Suarez, Chem. Rev. (Washington, D.C.) **102**, 3667 (2002).
[8] H. Zhao and S. V. Malhotra, Aldrichimica Acta **35**, 75 (2002).
[9] J. S. Willkes, Green Chem. **4**, 73 (2002).
[10] J. H. Davis, Jr., Chem. Lett. **33**, 1072 (2004).
[11] Y. Chauvin, L. Mußmann, and H. Olivier, Angew. Chem., Int. Ed. Engl. **34**, 2698 (1995).
[12] P. A. Z. Suarez, J. E. L. Dullius, S. Einloft, R. F. de Souza, and J. Dupont, Polyhedron **15**, 1217 (1996).
[13] C. E. Song and E. J. Roh, Chem. Commun. (Cambridge) **2000**, 837.
[14] W. Chen, L. Xu, C. Chatterton, and J. Xiao, Chem. Commun. (Cambridge) **1999**, 1247.
[15] C. de Bellefon, E. Pollet, and P. Grenouillet, J. Mol. Catal. A: Chem. **145**, 121 (1999).
[16] K. Jin, X. Y. Huang, L. Pang, J. Li, A. Appel, and S. Wherland, Chem. Commun. (Cambridge) **23**, 2872 (2002).
[17] M. Eckstein, P. Wasserscheid, and U. Kragl, Biotechnol. Lett. **24**, 763 (2002).
[18] A. L. Monteiro, F. K. Zinn, R. F. de Souza, and J. Dupont, Tetrahedron: Asymmetry **8**, 177 (1997).
[19] A. Hu, H. L. Ngo, and W. Lin, Angew. Chem., Int. Ed. **43**, 2501 (2004).
[20] A. Berthod, L. He, and D. W. Armstrong, Chromatographia **53**, 63 (2001).
[21] D. W. Armstrong, L. K. Zhang, L. F. He, and M. L. Gross, Anal. Chem. **73**, 3679 (2001).
[22] S. Carda-Broch, A. Berthod, and D. W. Armstrong, Rapid Commun. Mass Spectrom. **17**, 553 (2003).
[23] Z. B. Alfassi, R. E. Huie, B. L. Milman, and P. Neta, Anal. Bioanal. Chem. **377**, 159 (2003).
[24] D. McMorrow, W. T. Lotshaw, and G. A. Kenney-Wallace, IEEE J. Quantum Electron. **24**, 443 (1988).
[25] W. T. Lotshaw, D. McMorrow, N. Thantu, J. S. Melinger, and R. Kitchenham, J. Raman Spectrosc. **26**, 571 (1995).
[26] D. McMorrow and W. T. Lotshaw, Chem. Phys. Lett. **174**, 85 (1990).
[27] D. McMorrow and W. T. Lotshaw, J. Phys. Chem. **95**, 10395 (1991).
[28] S. Kinoshita, Y. Kai, T. Ariyoshi, and Y. Shimada, Int. J. Mod. Phys. B **10**, 1229 (1996).
[29] E. W. Castner, Jr. and M. Maroncelli, J. Mol. Liq. **77**, 1 (1998).
[30] N. A. Smith and S. R. Meech, Int. Rev. Phys. Chem. **21**, 75 (2002).
[31] B. J. Loughnane, R. A. Farrer, A. Scodinu, T. Reilly, and J. T. Fourkas, J. Phys. Chem. B **104**, 5421 (2000).
[32] R. A. Farrer and J. T. Fourkas, Acc. Chem. Res. **36**, 605 (2003).
[33] N. T. Hunt, A. A. Jaye, and S. R. Meech, J. Phys. Chem. B **107**, 3405 (2003).
[34] N. T. Hunt, A. A. Jaye, A. Hellman, and S. R. Meech, J. Phys. Chem. B **108**, 100 (2004).
[35] G. Giraud and K. Wynne, J. Am. Chem. Soc. **124**, 12110 (2002).
[36] G. Giraud, J. Karolin, and K. Wynne, Biophys. J. **85**, 1903 (2003).
[37] J. D. Eaves, C. J. Fecko, A. L. Stevens, P. Peng, and A. Tokmakoff, Chem. Phys. Lett. **376**, 20 (2003).
[38] H. Shirota and E. W. Castner, Jr., J. Am. Chem. Soc. **123**, 12877 (2001).
[39] B. R. Hyun, S. V. Dzyuba, R. A. Bartsch, and E. L. Quitevis, J. Phys. Chem. A **106**, 7579 (2002).
[40] J. Rajian, S. Li, R. Bartsch, and E. Quitevis, Chem. Phys. Lett. **393**, 372 (2004).
[41] G. Giraud, C. M. Gordon, I. R. Dunkin, and K. Wynne, J. Chem. Phys. **119**, 464 (2003).
[42] H. Cang, J. Li, and M. D. Fayer, J. Chem. Phys. **119**, 13017 (2003).
[43] A. M. Funston, E. Trofimovsky, K. Odynocki, M. N. Kobrak, and J. F.

Wishart (unpublished).
[44]P. Wasserscheid and T. Welton, *Ionic Liquids in Synthesis* (Wiley-VCH, Weinheim, 2003).
[45]D. R. MacFarlane, P. Meakin, J. Sun, N. Amini, and M. Forsyth, J. Phys. Chem. B **103**, 4164 (1999).
[46]N. L. Lancaster, P. A. Salter, T. Welton, and G. B. Young, J. Org. Chem. **67**, 8855 (2002).
[47]D. R. MacFarlane, J. Sun, J. Golding, P. Meakin, and M. Forsyth, Electrochim. Acta **45**, 1271 (2000).
[48]D. R. MacFarlane, S. A. Forsyth, J. Golding, and G. B. Deacon, Green Chem. **4**, 444 (2002).
[49]D. R. MacFarlane, J. Golding, S. Forsyth, M. Forsyth, and G. B. Deacon, Chem. Commun. (Cambridge) **2001**, 1430.
[50]P. P. Wiewior, H. Shirota, and E. W. Castner, Jr., J. Chem. Phys. **116**, 4643 (2002).
[51]M. J. Frisch, G. W. Trucks, H. B. Schlegel *et al.*, GAUSSIAN 03, Gaussian, Inc., Pittsburgh, PA, 2003.
[52]A. D. Becke, J. Chem. Phys. **98**, 5648 (1993).
[53]C. Lee, W. Yang, and R. G. Parr, Phys. Rev. B **37**, 785 (1988).
[54]N. Ito, S. Arzhantsev, M. Heitz, and M. Maroncelli, J. Phys. Chem. B **108**, 5771 (2004).
[55]B. Mennucci and J. Tomasi, J. Chem. Phys. **106**, 5151 (1997).
[56]B. Mennucci, E. Cances, and J. Tomasi, J. Phys. Chem. B **101**, 10506 (1997).
[57]See EPAPS Document No. E-JCPSA6-122-506519 for details of the GAUSSIAN 03 calculation results. Optimized geometries, electrostatic parameters, and rotational constants, and CHelpG charges are tabulated. This document can be reached via a direct link in the online article's HTML reference section or via the EPAPS homepage (http://www.aip.org/pubservs/epaps.html).
[58]B. J. Loughnane and J. T. Fourkas, J. Phys. Chem. B **102**, 10288 (1998).
[59]D. Kivelson and P. A. Madden, Annu. Rev. Phys. Chem. **31**, 523 (1980).
[60]G. R. Fleming, *Chemical Applications of Ultrafast Spectroscopy* (Oxford University Press, New York, 1986).
[61]J. T. Edwards, J. Chem. Educ. **47**, 261 (1970).
[62]Because the values for S of NTf_2^- and N- for NTf_2^- and DCA^- are not listed, the value for S is used as $2\times S=$and the value for N is tentatively used as >N-.
[63]J. N. Israelachvili, *Intermolecular and Surface Forces*, 2nd ed. (Academic, London, 1992).
[64]M. N. Kobrak and V. Znamenskiy, Chem. Phys. Lett. **395**, 127 (2004).
[65]C. J. Margulis, Mol. Phys. **102**, 829 (2004).
[66]R. Karmakar and A. Samanta, J. Phys. Chem. A **106**, 4447 (2002).
[67]R. Karmakar and A. Samanta, J. Phys. Chem. A **107**, 7340 (2003).
[68]D. Chakravarty, P. Harza, A. Chakravarty, D. Seth, and N. Sarkar, Chem. Phys. Lett. **381**, 697 (2003).
[69]S. Arzhantsev, N. Ito, M. Heitz, and M. Maroncelli, Chem. Phys. Lett. **381**, 278 (2003).
[70]J. A. Ingram, R. S. Moog, N. Ito, R. Biswas, and M. Maroncelli, J. Phys. Chem. B **107**, 5926 (2003).
[71]N. Ito, S. Arzhantsev, and M. Maroncelli, Chem. Phys. Lett. **396**, 83 (2004).
[72]J. D. Holbrey, W. M. Reichert, and R. D. Rogers, J. Chem. Soc. Dalton Trans. **2004**, 2267.
[73]M. Castriota, T. Caruso, R. G. Agostino, E. Cazzanelli, W. A. Henderson, and S. Passerini, J. Phys. Chem. A **109**, 92 (2005).
[74]I. Rey, P. Johansson, J. Lindgren, J. C. Lassegues, J. Grondin, and L. Servant, J. Phys. Chem. A **102**, 3249 (1998).
[75]B. J. Loughnane, A. Scodinu, R. A. Farrer, J. T. Fourkas, and U. Mohanty, J. Chem. Phys. **111**, 2686 (1999).
[76]D. McMorrow, N. Thantu, V. Kleiman, J. S. Melinger, and W. T. Lotshaw, J. Phys. Chem. A **105**, 7960 (2001).
[77]D. McMorrow, W. T. Lotshaw, J. S. Melinger, and V. Kleiman, ACS Symp. Ser. **820**, 14 (2002).
[78]Y. Tanimura and S. Mukamel, J. Chem. Phys. **99**, 9496 (1993).
[79]S. Mukamel, *Principles of Nonlinear Optical Spectroscopy* (Oxford University Press, New York, 1995).
[80]Y. J. Chang and E. W. Castner, J. Phys. Chem. **98**, 9712 (1994).
[81]Y. J. Chang and E. W. Castner, Jr., J. Phys. Chem. **100**, 3330 (1996).
[82]N. A. Smith, S. Lin, S. R. Meech, and K. Yoshihara, J. Phys. Chem. A **101**, 3641 (1997).
[83]N. A. Smith, S. Lin, S. R. Meech, H. Shirota, and K. Yoshihara, J. Phys. Chem. A **101**, 9578 (1997).
[84]H. Shirota, K. Yoshihara, N. A. Smith, S. Lin, and S. R. Meech, Chem. Phys. Lett. **281**, 27 (1997).
[85]N. A. Smith and S. R. Meech, J. Phys. Chem. A **104**, 4223 (2000).
[86]N. T. Hunt and S. R. Meech, J. Chem. Phys. **120**, 10828 (2004).
[87]S. Palese, J. T. Buontempo, L. Schlling, W. T. Lotshaw, Y. Tamimura, S. Mukamel, and R. J. Dwayne Miller, J. Phys. Chem. **98**, 12466 (1994).
[88]S. Palese, L. Schilling, R. J. D. Miller, P. R. Staver, and W. T. Lotshaw, J. Phys. Chem. **98**, 6308 (1994).
[89]M. Cho, M. Du, N. F. Scherer, G. R. Fleming, and S. Mukamel, J. Chem. Phys. **99**, 2410 (1993).
[90]P. Bartolini, M. Ricci, R. Trroe, R. Righini, and I. Santa, J. Chem. Phys. **110**, 8653 (1999).
[91]H. Shirota, J. Chem. Phys. **122**, 044514 (2005).
[92]P. A. Madden and T. I. Cox, Mol. Phys. **43**, 287 (1981).
[93]P. A. Madden, in *Ultrafast Phenomena IV*, edited by A. H. Auston and K. B. Eisenthal (Springer, Berlin, 1984), Vol. 38, p. 244.
[94]L. C. Geiger and B. M. Ladanyi, J. Chem. Phys. **89**, 6588 (1988).
[95]L. C. Geiger and B. M. Ladanyi, Chem. Phys. Lett. **159**, 413 (1989).
[96]S. Ryu and R. M. Stratt, J. Phys. Chem. B **108**, 6782 (2004).
[97]P. K. Chowdhury, M. Halder, L. Sanders, T. Calhoun, J. L. Anderson, D. W. Armstrong, X. Song, and J. W. Petrich, J. Phys. Chem. B **108**, 10245 (2004).
[98]M. N. Kobrak and N. Sandalow, in *Molten Salts XIV*, edited by R. A. Mantz (The Electrochemical Society, Pennington, NJ, 2005).
[99]T. I. Morrow and E. J. Maginn, J. Phys. Chem. B **106**, 12807 (2002).
[100]J. de Andrade, E. S. Boes, and H. Stassen, J. Phys. Chem. B **106**, 13344 (2002).
[101]C. G. Hanke, S. L. Price, and R. M. Lynden-Bell, Mol. Phys. **99**, 801 (2001).
[102]T. Y. Yan, C. J. Burnham, M. G. Del Popolo, and G. A. Voth, J. Phys. Chem. B **108**, 11877 (2004).
[103]M. G. Del Popolo and G. A. Voth, J. Phys. Chem. B **108**, 1744 (2004).
[104]C. J. Margulis, H. A. Stern, and B. J. Berne, J. Phys. Chem. B **106**, 12017 (2002).
[105]V. Znamenskiy and M. N. Kobrak, J. Phys. Chem. B **108**, 1072 (2004).
[106]C. G. Hanke, A. Johansson, J. B. Harper, and R. M. Lynden-Bell, Chem. Phys. Lett. **374**, 85 (2003).
[107]C. G. Hanke and R. M. Lynden-Bell, J. Phys. Chem. B **107**, 10873 (2003).
[108]J. B. Harper and R. M. Lynden-Bell, Mol. Phys. **102**, 85 (2004).
[109]Y. Shim, J. S. Duan, M. Y. Choi, and H. J. Kim, J. Chem. Phys. **119**, 6411 (2003).